Carbohydrate Polymer Technologies and Applications 14 (2026) 101166

Contents lists available at ScienceDirect

Carbohydrate Polymer Technologies and Applications

journal homepage: www.sciencedirect.com/journal/carbohydrate-polymer-technologies-and-applications

Soil and enzyme-driven degradation mechanisms of alginate- and chitosan-based biocomposite films

Miša Mojca Cajnko [a,*], Kostadin Mitkov [a], Blaž Likozar [a], Blaž Stres [a,b,c,d]

[a] National Institute of Chemistry, Slovenia
[b] Faculty of Civil and Geodetic Engineering, University of Ljubljana, Ljubljana, Slovenia
[c] Faculty of mechanical engineering, University of Ljubljana, Ljubljana, Slovenia
[d] Institute Jožef Stefan, Ljubljana, Slovenia

ARTICLE INFO

Keywords:
Biocomposite films
Chitosan
Alginate
Biodegradation
Enzymatic depolymerization
Plant toxicity

ABSTRACT

We prepared biocomposite films based on alginate (A) and chitosan (Ch) reinforced with cellulose nanocrystals (CNC) or acetylated CNC (mCNC). Their behaviour in native forest soil was evaluated using two set-ups: film on top of soil (TOP) and film between two soil layers (MID). Under the tested conditions, all films reached complete disappearance, with the TOP set-up degrading notably slower (ca. 80–100 days) than the MID set-up (ca. 30 days). Ch-based films disappeared faster than A-based films in the TOP set-up. To obtain mechanistic insight, the films were exposed in vitro to four soil-associated enzymes: lipase (Lip), cellulase (Cel), laccase (Lac), and alcohol dehydrogenase (ADH). Lip and Cel produced the highest release of reducing sugars, whereas Lac and ADH showed only minor effects. ATR-FTIR analysis of residual chitosan-based films showed spectral changes consistent with chemical modification/depolymerization, but not direct proof of specific bond cleavage. Finally, the potential phytotoxicity of degradation products was assessed using barley seeds, but no major inhibitory effect on germination or growth was observed. Overall, the results support the environmental disappearance and enzymatic susceptibility of these biocomposite films, while also highlighting the qualitative nature of the soil assay and the need for future mineralization-focused studies.

1. Introduction

Plastic production continues to rise globally, while the environmental persistence of conventional petroleum-based plastics and their fragmentation products remains a major ecological concern (Dong et al., 2020; Gajendiran et al., 2016; Isangedighi et al., 2020; Rosenboom et al., 2022; Stapleton, 2019). For this reason, polysaccharide-based materials are being intensively investigated as renewable and potentially biodegradable alternatives, especially for packaging and other short-life applications. Recent reviews highlight alginate, chitosan and cellulose-derived nanomaterials as particularly attractive building blocks because of their abundance, film-forming ability, tuneable intermolecular interactions and broad formulation space (Guzmán-Pincheira et al., 2025; Li et al., 2024; Xie et al., 2024).

For such materials, however, "biodegradability" cannot simply be treated as an intrinsic property based on the polymer alone. The observed rate and extent of degradation depend on moisture, oxygen availability, ion composition, film structure, accessibility of hydrolysable bonds, and the composition and metabolic state of the surrounding microbiome. In soil, biodegradation is further shaped by the local enzymatic repertoire, which varies across habitats and soils (Abou-Zeid et al., 2001; Fujisawa et al., 2001; Hung et al., 2016; Kim et al., 2020; Mukherjee et al., 2011; Pathak & Navneet, 2017; Rinta-Kanto et al., 2016; Vaksmaa et al., 2021; Yoon et al., 2012). Therefore, studies that combine environmentally relevant soil exposure with simplified in vitro enzyme tests can be useful for distinguishing between disappearance behavior in complex matrices and polymer susceptibility to specific enzyme classes.

In our previous works, we prepared biocomposite films based on natural polysaccharides, alginate and chitosan and studied their degradation in an aqueous medium (Oberlintner et al., 2023; Vidmar et al., 2023). In the present study, we extend that work to a native forest-soil microcosm and to selected enzyme-mediated reactions (Fig. 1). We specifically compare neat A and Ch films with their CNC- and mCNC-containing counterparts, and we assess possible effects of the resulting degradation products on barley germination and growth.

* Corresponding author at: Hajdrihova 19, 1000 Ljubljana, Slovenia.
E-mail address: misa.cajnko@ki.si (M.M. Cajnko).

https://doi.org/10.1016/j.carpta.2026.101166

Available online 25 May 2026

Importantly, the soil experiment was designed as a native-soil disappearance assay under environmentally relevant conditions, not as a standardized ASTM/ISO mineralization test. Accordingly, the mechanistic interpretation of the enzyme assays is based on reducing-sugar release and ATR-FTIR trends and is discussed cautiously.

Recent literature also shows continued expansion of alginate- and chitosan-based films for packaging and other transient applications, but comparatively fewer studies directly connect film disappearance in soil with enzyme-level observations on the same material system (Guzmán-Pincheira et al., 2025; Li et al., 2024; Metha et al., 2024).

2. Materials and methods

2.1. Materials

Lipase from *Rhizopus oryzae* (Sigma-Aldrich); Laccase from *Trametes versicolor* (Sigma-Aldrich); Cellulase from *Aspergillus niger* (Sigma-Aldrich); Alcohol dehydrogenase from *Saccharomyces cerevisiae* (Sigma-Aldrich); Chitosan (300 – 1000 cps; Glentham Life sciences); Alginic acid sodium salt from brown algae, medium viscosity (Sigma-Aldrich); Lactic acid (Sigma-Aldrich); Glycerol (Pharmachem); Cellulose nanocrystals (Nanocrystacell); Sodium azide (Sigma-Aldrich); 3,5-Dinitrosalicylic acid (Sigma-Aldrich); Potassium sodium tartrate tetra-hydrate (Sigma-Aldrich); Sodium hydroxide (Sigma-Aldrich); D(+)-Glucose (Sigma-Aldrich); Trizma® base (Merck); Hydrochloric acid (Sigma-Aldrich); Di-sodium hydrogen phosphate dihydrate (Fluka); Sodium dihydrogen phosphate dihydrate (Merck).

Commercial CNCs were used as supplied by the manufacturer and then freeze-dried before use. Detailed supplier specifications such as size distribution, aspect ratio, zeta potential, and sulfate group content were not independently re-measured in the present study; the modified CNC (mCNC) was prepared as described previously by Vidmar et al. (Vidmar et al., 2023).

2.2. Methods

2.2.1. Preparation of biocomposite films

Cellulose nanocrystals (CNC) were first freeze dried. The alginate (A)-based biocomposite films were prepared by mixing 19.5 g alginate and 2.9 g glycerol in 650 mL of distilled water (18.2 MΩ·cm). To improve homogenization, alginate was first dissolved in approximately half of the water under magnetic stirring at 300 rpm. The remaining water was then added, followed by glycerol, and the mixture was stirred at room temperature for 2 h homogenous. The mixture was then divided into three approximately equal portions (ca. 200 mL each). CNC or mCNC (150 mg) was added to the first and second portion, respectively, and dispersed by circular stirring at 600 rpm for 3 min using an Ultra-Turrax homogenizer (Ika, Staufen, Germany). No nanocellulose was added to the third portion. After degassing overnight, the mixtures were cast onto Petri dishes (12 × 12 cm; 50 g per dish) and dried in a ventilated dehydrator (Hendi, Germany) at 40 °C for 24 h.

The chitosan (Ch)-based biocomposite films were prepared by mixing 9.75 g chitosan, 2.93 g glycerol, 7.69 g lactic acid and 650 mL of distilled water (18.2 MΩ·cm). Lactic acid was included to protonate chitosan amino groups and enable dissolution and homogeneous film formation. Chitosan and glycerol were first combined in a beaker, after which lactic acid was added dropwise. Water was then added and the suspension was stirred at 300 rpm for 24 h to ensure complete dissolution. To remove impurities, the chitosan solution was vacuum-filtered through four layers of medical gauze. The filtered mixture was divided into three portions (ca. 200 mL each). CNC or mCNC (90 mg) was added to the first and second portion, respectively, and dispersed by circular stirring at 600 rpm for 3 min using an Ultra-Turrax homogenizer. No nanocellulose was added to the third portion. After degassing overnight, the mixtures were cast onto Petri dishes (12 × 12 cm; 50 g per dish) and dried at 40 °C for 24 h.

2.2.2. Soil degradation

Soil was collected from Golovec hill forest (Ljubljana, Slovenia) after removing the uppermost plant-litter layer; only the mineral soil down to 15 cm depth was retained. The soil was sieved through a 3 mm sieve to remove coarse debris. Active and passive pH were measured as 5.7 and 7.1, respectively, as described previously (Food & Agriculture Organization, 2021). Water was then added to obtain moisture content of approximately 30 %. Films were cut into 3 × 3 cm pieces and incubated in two configurations: on top of the soil (TOP) or between two soil layers (MID). The Petri dishes were weighed regularly so that evaporative water loss could be replenished every 2–3 days. Lids were used to slow water loss while still allowing gas exchange. Samples were incubated at 20 °C. The endpoint of the soil assay was the disappearance of visible film fragments. This experiment was intended as a qualitative native-soil disappearance test rather than a standardized mineralization assay; gravimetric mass-loss measurements were not attempted because hydrated films swelled and became strongly associated with adhered soil particles, preventing reproducible recovery and weighing. Images of the films were taken every few days.

An additional experiment was performed with A film. The film (3 × 3 cm) was put on top of the soil (TOP set up) and a small lump of soil was put on top of it (MID set up). The degradation of the film was monitored until there was no visible film fragments underneath the lump of soil.

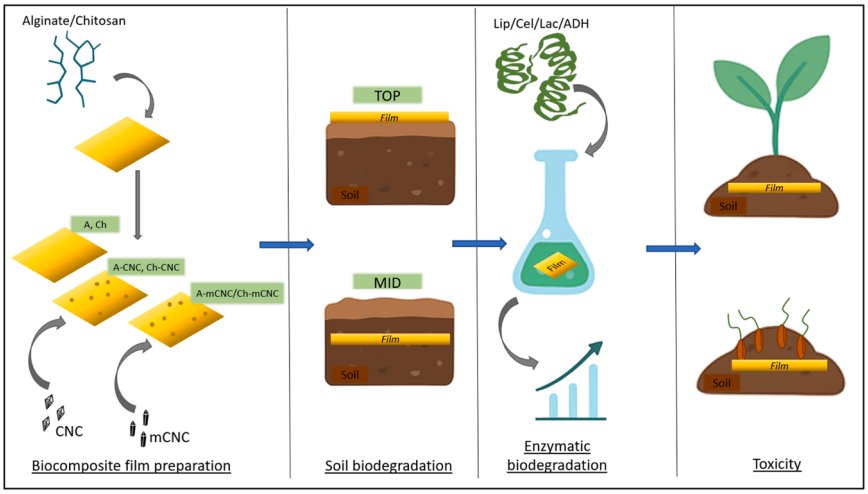

Fig. 1. Schematic representation of the experimental process.

2.2.3. In vitro enzymatic degradation

The in vitro enzymatic degradation of biocomposite films was carried out by incubating 2 × 2 cm film pieces in 5 mL of enzyme solutions at room temperature for 48 h. Lipase (Lip), cellulase (Cel), and laccase (Lac) were each used at 70 μM, and alcohol dehydrogenase (ADH) at 35 μM, in 100 mM phosphate buffer at pH 6 or 7. Lipase and cellulase were selected as hydrolytic enzymes relevant to polysaccharide-containing matrices, laccase as a common soil-associated oxidative enzyme, and ADH as an exploratory comparator related to dehydrogenase-rich soil metabolism rather than as an established polysaccharide depolymerase (Camiña et al., 1998; Fashogbon et al., 2021; Gu et al., 2009; Ryo et al., 2023; Sethi et al., 2013; Zhao et al., 2019) Enzymatic action was evaluated in the liquid phase by the DNS assay and in the solid phase by ATR-FTIR when recoverable solid residue remained.

For Lip and Cel, higher concentrations of 190 μM were also tested. For both Lip and Cel (70 and 190 μM concentrations), 96 h reactions were also tested. These reactions were carried out at pH 6 with Ch- and A-films, with the addition of 0.002 % of sodium azide (NaAz). Control samples contained the respective buffer without enzyme. Samples were taken at 0, 24, 48, 72 and 96 h, and the liquid fraction analysed using the DNS method.

An additional experiment was carried out with Lip and Cel. Ch films were incubated with 70 and 190 μM enzyme in 100 mM phosphate buffer (pH 6) for 48 h. After the incubation, the enzyme solution was removed and a fresh enzyme solution added to the remaining film or film figments. This procedure was repeated for a total of 4 cycles. Samples were taken at 0, 24 and 48 h for each cycle and the liquid fraction analysed using the DNS method. In reaction mixtures containing film fragments, 1 mL of mixture was taken and centrifuged, to separate the fragments from the solution. The samples for the DNS test were taken from the supernatant, and the remaining solution and film fragments were returned to the reaction mixture.

2.2.3.1. FT-IR analysis. After 48 h of in vitro enzymatic treatment, the remaining film fragments were removed, washed thoroughly with distilled water (18.2 MΩ·cm), dried at 40 °C for 24 h, and analysed by ATR-FTIR using a PerkinElmer spectrometer equipped with a UATR Two attachment. Spectra were recorded at 23 ± 1 °C over 4000–400 cm^{-1} with a resolution of 1 cm^{-1} and 64 scans. Three parallel spectra were collected per sample. For alginate-based films, recoverable solid residue was generally not available because the films dissolved rapidly upon contact with aqueous buffer; accordingly, ATR-FTIR interpretation is restricted to the chitosan-based residues.

2.2.3.2. Determination of the reducing sugar concentration. Two 100 μL aliquots were taken from each reaction mixture at each time point (0, 24 and 48 h; and additionally 72 and 96 h where applicable) and mixed with 200 μL DNS reagent as described previously (Hernández-López et al., 2020). After incubation at 95 °C for 5 min, 200 μL of each sample was transferred to a 96-well plate and absorbance was measured at 540 nm using a BioTek Synergy H1 microplate reader. Where required, additional dilution was performed with distilled water. Reducing sugar concentration was determined from a glucose calibration curve (0, 0.1, 0.5, 1, 3 and 6 mg mL^{-1}). Reported DNS values therefore represent duplicate analytical measurements for each sampled reaction mixture.

2.2.4. Toxicity of degradation products

Barley (*Hordeum vulgare*) seeds suitable for sprouting and preparation of microgreens were obtained from a health food shop (GEO, Tovarna Zdrave Hrane). Two experimental set-ups were used. In the first, barley seeds were germinated on wet paper towels for 7 days at 20 °C, sprouts of comparable size were planted 3 mm deep in soil (10 sprouts per film type), and alginate or chitosan films were laid on the soil surface. In the second, non-germinated seeds were sown directly in soil 3 mm deep (40 seeds per film type). In both cases, a thin soil layer was placed above the sprouts/seeds so that the films were positioned on top of a 3 mm soil cover. Plant size was measured in both experiments, and sprouted seed number (viability) was recorded in the second experiment. This test was used as a screening assay for gross phytotoxicity and did not include additional physiological endpoints such as root biomass, chlorophyll content or biochemical stress markers.

3. Results and discussion

3.1. Soil disappearance of biocomposite films as simulation of degradation in nature

Soil disappearance of the biocomposite films was assessed in forest soil using TOP and MID configurations. The experiment was followed until no visible film residue remained. Fig. 2 shows the first 20 days of the process. Under the tested conditions, all MID films reached complete visible disappearance by approximately day 30. Ch-based films visibly swelled and formed a firm gel-like structure, whereas A-based films became opaque, rigid and apparently dry to the touch. The TOP films disappeared more slowly: Ch-based films required approximately 80 days and A-based films approximately 100 days. No clear difference in disappearance time was observed between neat films and CNC- or mCNC-containing films within the same polymer family.

An additional experiment combining the TOP and MID configurations (Fig. S1) gave the same qualitative trend. When an A-film was placed on top of the soil and covered locally with a small lump of soil, the covered part (MID-like microenvironment) disappeared by approximately day 30, while a substantial fraction of the uncovered TOP region remained. These observations support the conclusion that contact area and local hydration strongly influence the visible disappearance of the films in soil.

The faster disappearance of MID films is most likely related to greater film–soil contact and a more favourable moisture regime. Both factors increase the accessible surface area for colonization and enzymatic attack. Although A-based films dissolve readily in bulk aqueous media, the ~30 % soil moisture used here was apparently insufficient to induce simple dissolution in soil. Instead, the alginate films became more rigid after soil contact, which may reflect ionic interactions or partial crosslinking with multivalent cations present in the soil matrix (Paques et al., 2014); however, the responsible ions were not measured, and specific assignments cannot be made from the present data alone. The faster disappearance of Ch-based films in TOP may reflect the broad occurrence of terrestrial microorganisms capable of utilizing chitin- or chitosan-like substrates (Crognale et al., 2022; Sidari et al., 2025), but this interpretation should remain cautious because only one forest soil was examined and its microbial composition and native enzyme activities were not characterized. Accordingly, the soil results should be interpreted as soil-specific disappearance behaviour rather than universal biodegradation kinetics.

3.2. In vitro enzymatic degradation of biocomposite films for mechanistic insight

To gain mechanistic insight under simplified conditions, the films were exposed to selected enzymes at pH 6 and 7. The enzyme panel was intentionally diverse and included hydrolytic (Lip, Cel) and oxidative/comparator (Lac, ADH) activities. The degree of depolymerization was estimated from the DNS assay, which measures reducing sugars/reducing ends in solution, while ATR-FTIR was used as a comparative tool for detecting chemical changes in the recoverable film residue. Neither method alone identifies the exact degradation products or proves a unique bond-cleavage pathway; therefore, the mechanistic interpretation below is limited to what can be supported by these datasets.

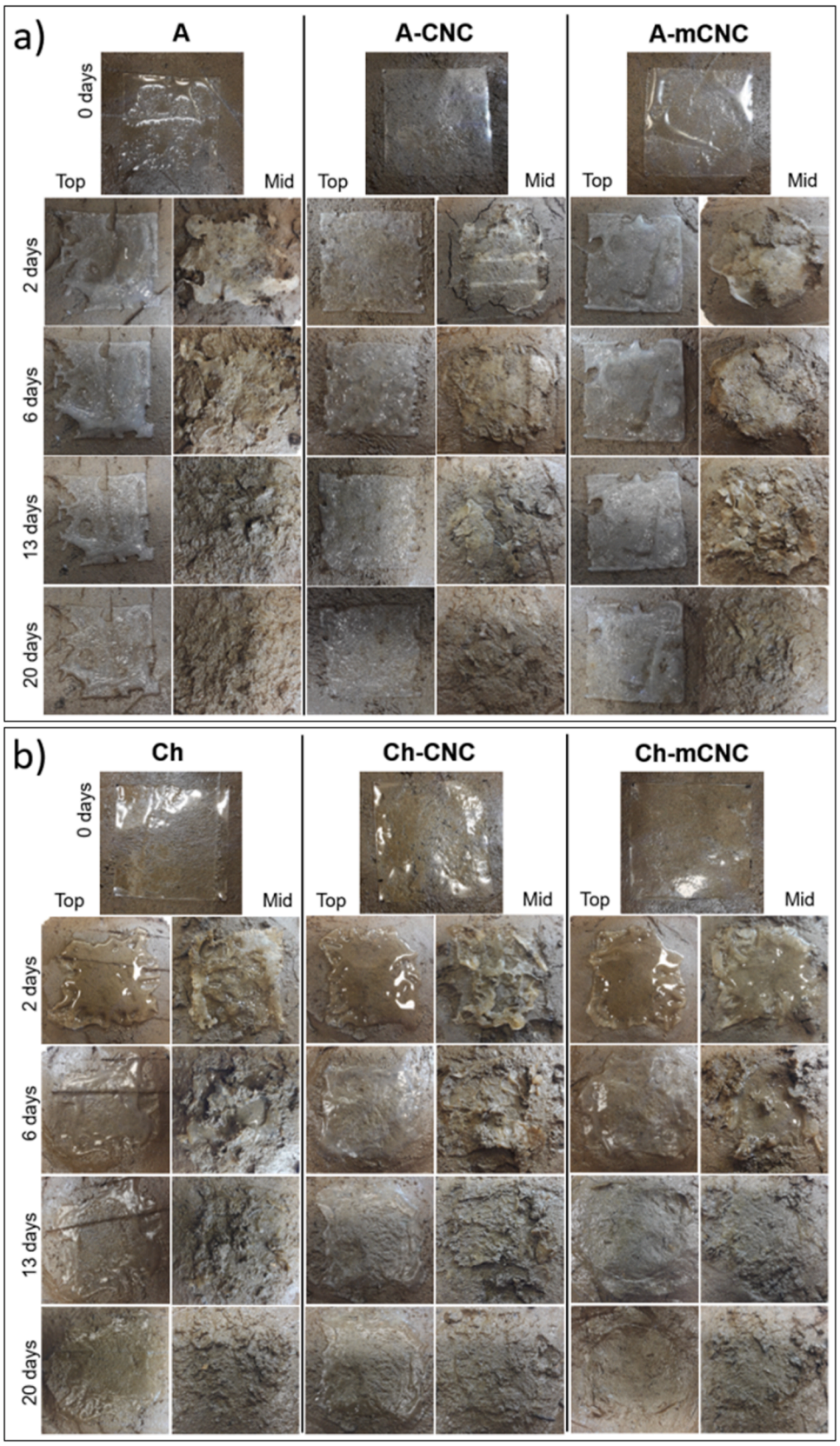

Fig. 2. Visual disappearance of alginate- (a) and chitosan-based (b) films in soil. A – alginate film; A-CNC – alginate film with cellulose nanocrystals; A-mCNC – alginate film with modified cellulose nanocrystals; Ch – chitosan film; Ch-CNC – chitosan film with cellulose nanocrystals; Ch-mCNC – chitosan film with modified cellulose nanocrystals; TOP – film on top of soil; MID – film between two soil layers.

3.2.1. ATR-FTIR analysis as a measure of changes in chemical bonds

The ATR-FTIR analysis was performed only on Ch-based films since the A-based films dissolved immediately upon contact with the aqueous reaction medium and no recoverable solid residue remained for analysis. All enzymes were tested at 70 μM concentration, except ADH, which was tested at 35 μM concentration due to the enzyme's large size which would require a substantial amount of mass. The ATR-FTIR spectra of the films after enzymatic treatment at pH 6 and 7, are presented in Fig. 3, and are used here as comparative evidence of chemical changes in the residual chitosan-based material, not as direct proof of specific scission events.

3.2.1.1. Lipase. After Lip treatment, Ch-based films showed only modest spectral changes relative to the buffer control. There were no changes detected in the main chitosan-associated bands (1639, 1570, and 1371 cm^{-1} (amide I–III) and 1060 cm^{-1} (C–O–C backbone)), indicating that the residual material retained the overall spectral signature of the parent polysaccharide matrix. An increas in OH groups, and the disappearance of the 1730 cm^{-1} (C = O) and 1150 cm^{-1} (ester) peaks was detected. Ch-CNC and Ch-mCNC films exhibited similar backbone stability, but Ch-CNC showed a loss of the 1730 cm^{-1} peak. There was also the appearance of a C = O peak. At pH 6, spectral changes were minimal. In Ch-CNC, increased C—H stretching and reduced OH intensity is observed, with a small 1750 cm^{-1} peak appearing.

These changes are consistent with partial chemical modification of the residual material, but they do not by themselves prove cleavage of a specific bond type. Because chitosan, cellulose and residual lactic-acid-related bands overlap in several diagnostic regions, it is difficult to

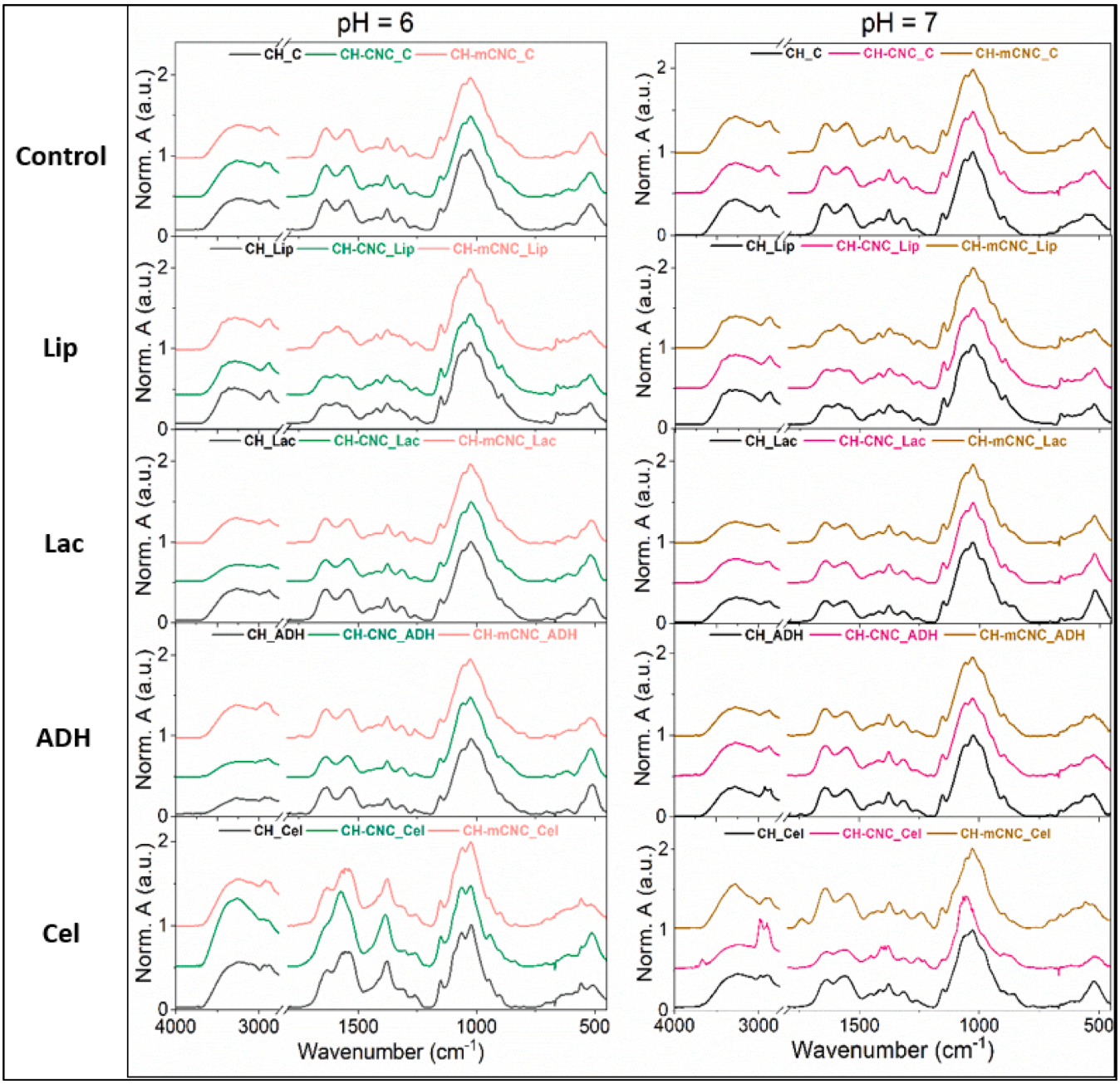

Fig. 3. FTIR spectra of chitosan-based biocomposite films after enzymatic degradation at 37 °C for 48 h. Ch – chitosan film; Ch-CNC – chitosan film with cellulose nanocrystals; Ch-mCNC – chitosan film with modified cellulose nanocrystals. C – control (buffer); Lip – lipase; Cel – cellulase; ADH – alcohol dehydrogenase; Lac – laccase.

assign these changes uniquely to one component of the composite. This is especially relevant for CNC- and mCNC-containing films.

Taken together, the FTIR and DNS results (Section 3.2.2 Determination reducing sugar concentration as measure of depolymerization) support the interpretation that lipase can promote partial depolymerization of these films under the tested conditions. However, the precise products and molecular-weight changes would need to be confirmed by orthogonal analyses such as SEC/GPC, LC-MS or NMR.

3.2.1.2. Laccase. Lac was included as a soil-associated oxidative enzyme (Zhao et al., 2019) for comparison rather than as a known polysaccharide-depolymerizing enzyme. In the present system, direct cleavage of alginate or chitosan backbones by laccase was not expected. Consistent with this, FTIR revealed no substantial spectral changes after laccase treatment, and the DNS assay also showed only minimal reducing sugar release. We therefore interpret laccase activity toward these films as negligible under the tested conditions.

3.2.1.3. Alcohol dehydrogenase. ADH was included as an exploratory comparator because dehydrogenase-type activity is widely associated with soil microbial metabolism (Camiña et al., 1998; Gu et al., 2009; Kaczyńska et al., 2015). However, ADH is not an established depolymerizing enzyme for alginate or chitosan, and its selection should therefore be viewed as exploratory rather than mechanism-driven.

Some spectral differences were observed after ADH exposure, mainly in regions associated with OH-, amine- and C = O-containing groups. Because these changes were small, inconsistent across film types, and not accompanied by substantial reducing-sugar release (DNS assay), they cannot be used as evidence of meaningful polysaccharide depolymerization. Additional targeted oxidation-product analysis would be required before any stronger mechanistic conclusion could be justified.

3.2.1.4. Cellulase. Cellulase catalyses the hydrolysis of cellulose and related polysaccharides and has also been reported to act, to varying extents, on chitosan-containing substrates (Xia et al., 2008). In the present study, cellulase was therefore used as a plausible hydrolytic enzyme for the cellulose-containing composites and for possible nonspecific activity toward the chitosan matrix.

In Ch films, an increased amide I and II (1636 cm^{-1} and 1541 cm^{-1}, respectively) was observed, while the polysaccharide backbone remained largely intact. In Ch-CNC films at pH 6, an increase in OH/NH intensity and a significant decrease in the 1060 cm^{-1} backbone peak was detected, and at pH 7, C–H vibrations increased. In Ch-mCNC films, changes at 1380 cm^{-1} (pH 6) and the appearance of a 1750 cm^{-1} C = O peak (pH 7) were detected.

These changes are consistent with chemical modification and partial depolymerization of the residual material. However, they are not sufficient to claim cellulase-induced deacetylation or a unique cleavage pattern. The combined FTIR and DNS results support cellulase activity toward the films, but detailed product identification would again require complementary analytical methods.

3.2.2. Determination reducing sugar concentration as measure of depolymerization

The DNS method was used to estimate the degree of depolymerization by quantifying reducing sugars/reducing ends released into solution (Saqib & Whitney, 2011). This test has previously been used to determine the depolymerization of chitosan by various enzymes (Huafei et al., 2024). This assay is sensitive to monomeric and some oligomeric hydrolysis products (Saqib & Whitney, 2011), however the test does not provide molecular-weight distributions or identify individual structures. It was therefore used here as a comparative indicator of enzyme-driven depolymerization rather than as a complete product-analysis method.

First, all films were subjected to treatment with 70 μM Lip, Cel and Lac or 35 μM ADH. The lower ADH concentration was used due its large molecular size. Fig. 4 shows depolymerization based on reducing sugar concentrations after treatment of Ch-based films at pH 7 and 6. Lac and ADH had little to no effect on all Ch-based films at both pH values, whereas Lip and Cel induced a significant release of reducing sugars. In Cel-catalysed reactions, reducing sugar concentrations in Ch films increased from ~0.6 mg mL^{-1} to ~0.9–1.0 mg mL^{-1} after 24 h and remained relatively stable up to 48 h at both pH values. In Lip-catalysed reactions, concentrations rose from ~0.02–0.03 mg mL^{-1} to ~0.8–1.2 mg mL^{-1} after 24 h, followed by a decrease or stabilization at 48 h. Similar trends were observed for all Ch-based films (Ch, Ch-CNC, and Ch-mCNC). No sugar release was detected in control samples, confirming the stability of the films under the tested conditions.

Fig. 5 shows depolymerization of A-based films based on reducing sugar concentrations after enzymatic treatment at pH 7 and 6. ADH and Lac exhibited minimal activity, releasing ≤0.1 and ≤0.2 mg mL^{-1} sugars at pH 7, respectively, with even lower activity at pH 6. Treatment of A-films with Lip at pH 7, induced notable increase of reducing sugars from up to ~0.6 mg mL^{-1} in A films and to ~0.8–1.0 mg mL^{-1} in A-CNC and A-mCNC films in 24 h, followed by stabilization.

At pH 6, reducing sugar concentrations rose from 1 mg mL^{-1} to 2 mg mL^{-1} in 24 h and decreased to 1.3 mg mL^{-1} after 48 h. Similar measurements were obtained for A-CNC and A-mCNC films.

In Cel-catalysed reactions at pH 7, the initial sugar concentration was 0.3 mg mL^{-1} for all A-based films. With A-films, the concentration dropped to 0.2 mg mL^{-1} after 24 h and remained stable, and for A-CNC and A-mCNC films, it increased to 0.4 mg mL^{-1} in 24 h and then slightly decreased to 0.3 mg mL^{-1} after 48 h. At pH 6, Lip treatment of all A-based films resulted in initial reducing sugar concentration of 0.7 mg mL^{-1}, which then gradually decreased to 0.5 mg mL^{-1} in 48 h.

Since both enzymes showed notable activity on alginate and chitosan polymers, we tested these enzymes at a higher concentration (190 μM) to assess whether complete film degradation could be achieved. Fig. 6 presents the reducing sugar concentrations following treatment of Ch- and A-films with 190 μM Lip or Cel at pH 7 and 6. For Ch-films, Cel at pH 7 produced 2.3 mg mL^{-1} of reducing sugars after 24 h, decreasing to 2.0 mg mL^{-1} after 48 h. At pH 6, the concentration reached 2.2 mg mL^{-1} after 24 h, and remained stable afterwards. In contrast, Lip showed higher activity. At pH 7, reducing sugars increased from the initial 2.4 mg mL^{-1} to 4.6 mg mL^{-1} after 24 h, followed by a slight decrease to 4.4 mg mL^{-1} after 48 h. At pH 6, reducing sugars values were even higher. Starting at 2.7 mg mL^{-1}, then increasing to 5.6 mg mL^{-1} in 24 h and stabilizing at 5.5 mg mL^{-1} after 48 h.

For A-films, treatment with Lip at pH 7 resulted in initial reducing sugar concentration of 3.0 mg mL^{-1}, which rose to 3.5 mg mL^{-1} in 24 h before declining to 2.5 mg mL^{-1} after 48 h. At pH 6, concentrations rose from the initial 2.4 mg mL^{-1} to 4 mg mL^{-1} in 24 h and remained stable after 48 h. In contrast, treatment with Cel at pH 7 resulted in initial reducing sugar concentration of 1.5 mg mL^{-1}, which dropped to 0.4 and 0.3 mg mL^{-1} after 24 and 48 h, respectively. At pH 6, the initial reducing sugar concentration started at 1.7 mg mL^{-1}, then slightly increased to 1.8 mg mL^{-1} after 24 h and then declined to 0.7 mg mL^{-1} after 48 h. Similar trends were observed for other Ch- and A-based films (Ch-CNC, Ch-mCNC, A-CNC and A-mCNC) with both enzymes (Fig. S3 and S4).

Chitosan is insoluble in neutral and alkaline aqueous solutions, but becomes soluble under acidic conditions (<pH 6.5) (Kumar et al., 2004). Although the Ch-based films did not dissolve in solution with pH 6, partial loosening of the matrix may have increased enzyme accessibility. In contrast, A-based films dissolved rapidly in the reaction medium at both pH values, which made alginate chains immediately available for solution-phase attack and likely contributed to the comparatively high DNS signals measured in Lip-containing mixtures.

Previous literature shows that enzymatic activity toward chitosan/cellulose-rich systems depends strongly on enzyme source, substrate presentation and reaction medium (Poshina et al., 2018; Xia et al., 2008). In our experiments, Lip and Cel generated the strongest DNS response, whereas Lac and ADH did not. For alginate, the present data

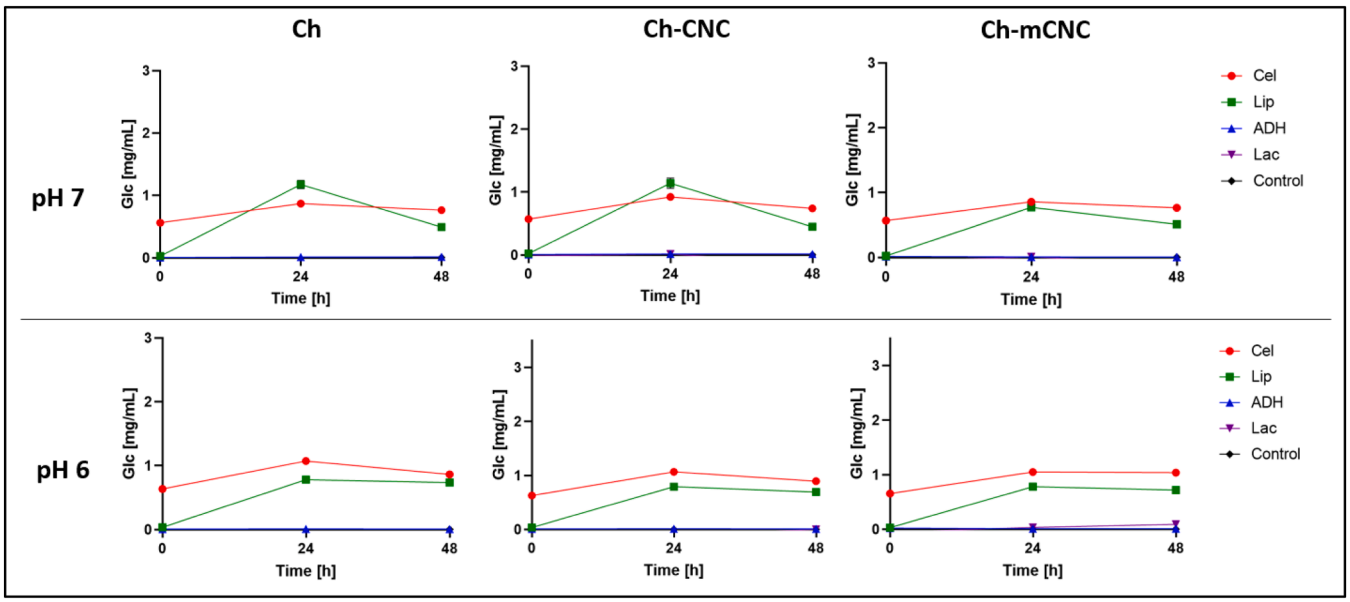

Fig. 4. Reducing sugar concentration after enzymatic treatment of chitosan-based films at pH 7 and 6. Ch – chitosan film; Ch-CNC – chitosan film with cellulose nanocrystals; Ch-mCNC – chitosan film with modified cellulose nanocrystals; Lip – lipase (70 μM); Cel – cellulase (70 μM); Lac – laccase (70 μM); ADH – alcohol dehydrogenase (35 μM). Variability is shown as standard deviation of duplicate analytical DNS measurements (error bars are not visible when SD was below 10 %).

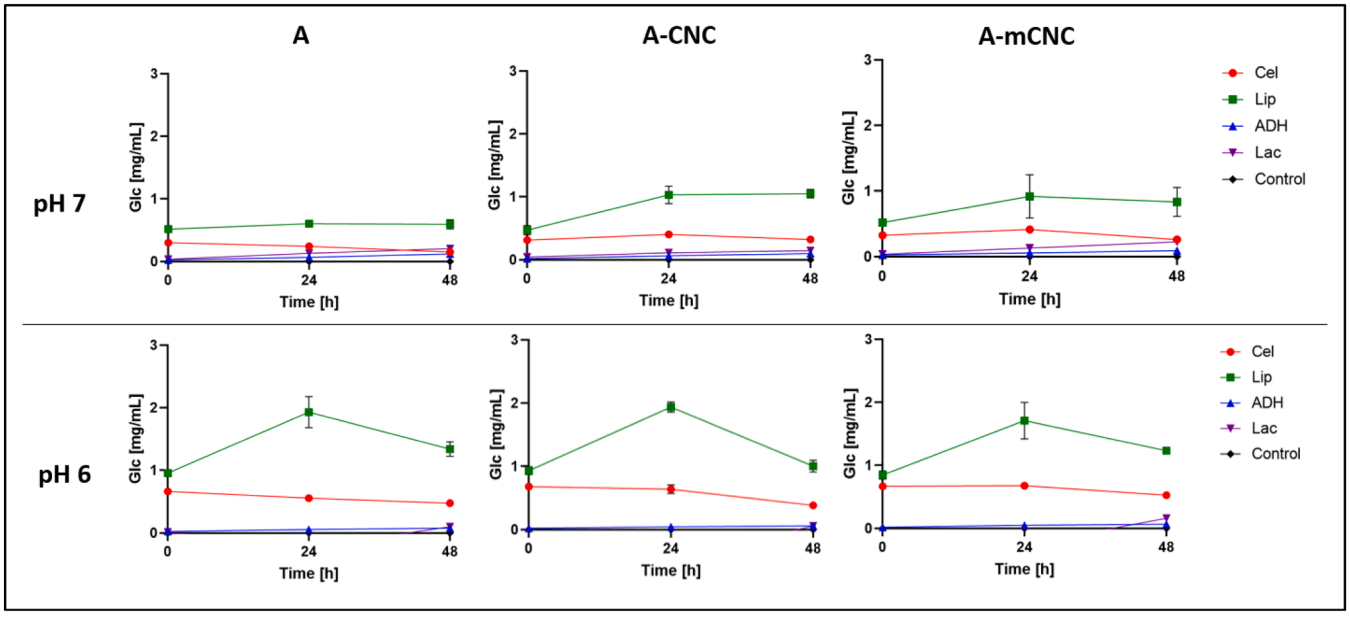

Fig. 5. Reducing sugar concentration after enzymatic treatment of chitosan-based films at pH 7 and 6. Ch – chitosan film; Ch-CNC – chitosan film with cellulose nanocrystals; Ch-mCNC – chitosan film with modified cellulose nanocrystals; Lip – lipase (70 μM); Cel – cellulase (70 μM); Lac – laccase (70 μM); ADH – alcohol dehydrogenase (35 μM). Variability is shown as standard deviation of duplicate analytical DNS measurements (error bars are not visible when SD was below 10 %).

indicate susceptibility of the dissolved film matrix under the chosen reaction conditions, but they do not establish a definite alginate-degradation pathway for either Lip or Cel. Likewise, although the changes in the FTIR spectra in Ch-based residues are compatible with depolymerization, they should not be interpreted as definitive proof of glycosidic-bond cleavage without additional product analysis.

Our measurements showed that reducing sugar concentrations sometimes decreased after 48 h in Lip- and Cel-containing systems (Fig. 6). One plausible explanation was secondary microbial consumption of released sugars by residual microbiota associated with the film surface. To test this possibility, follow-up reactions were carried out in the presence of sodium azide (NaAz), which suppresses microbial growth. Additionally, the reactions were also performed with higher enzyme concentrations, all of which allowed us to examine the time course of sugar release more clearly. Ch- and A-films were incubated in buffer pH 6 with or without Lip or Cel (70 and 190 μM) and with added sodium azide (NaAz). The reactions mixtures were incubated for 96 h, and reducing sugar concentration determined at the beginning and then every 24 h (Fig. 7). In the presence of NaAz, the DNS signal remained stable after reaching a plateau, supporting the interpretation that the earlier signal decrease was due mainly to biological consumption of released sugars rather than repolymerization or chemical loss. The maximum reducing sugar concentration released from Ch-films was 1 mg mL^{-1} and 2 mg mL^{-1} with 70 μM Cel and Lip, and 3 mg mL^{-1} and 6 mg

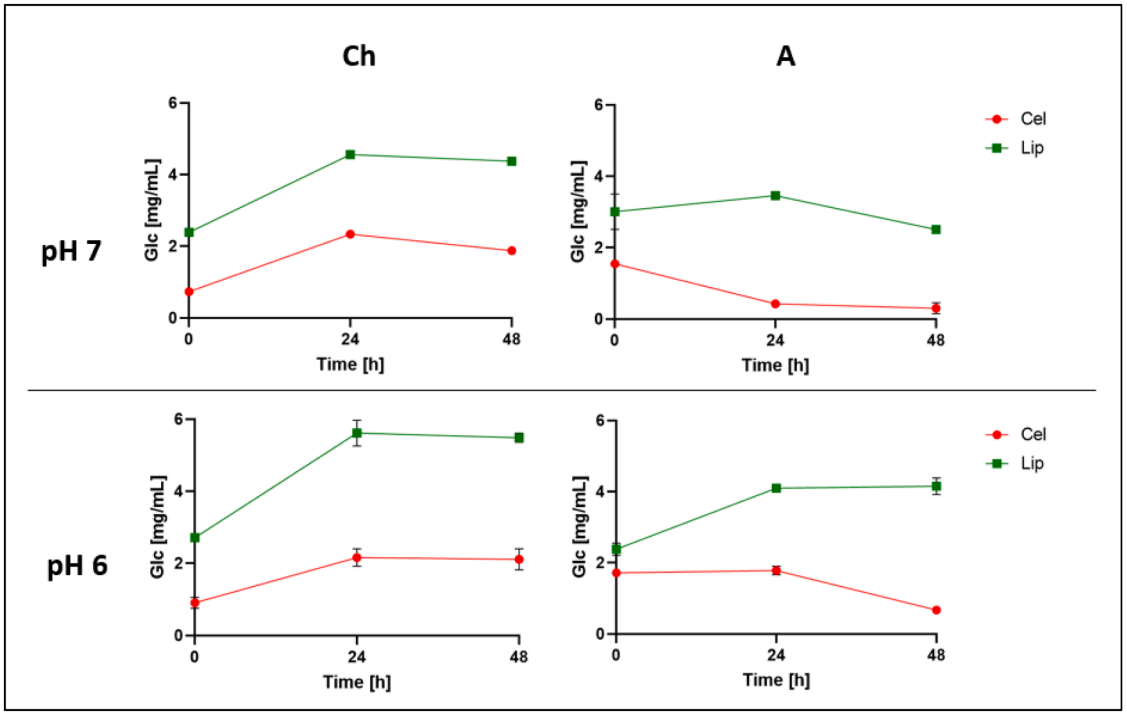

Fig. 6. Reducing sugar concentration after degradation of chitosan and alginate films with 190 μM lipase and cellulase at pH 7 and 6. A – alginate film; Ch – chitosan film; Lip – lipase; Cel – cellulase. Variability is shown as standard deviation of duplicate analytical DNS measurements (error bars are not visible when SD was below 10 %).

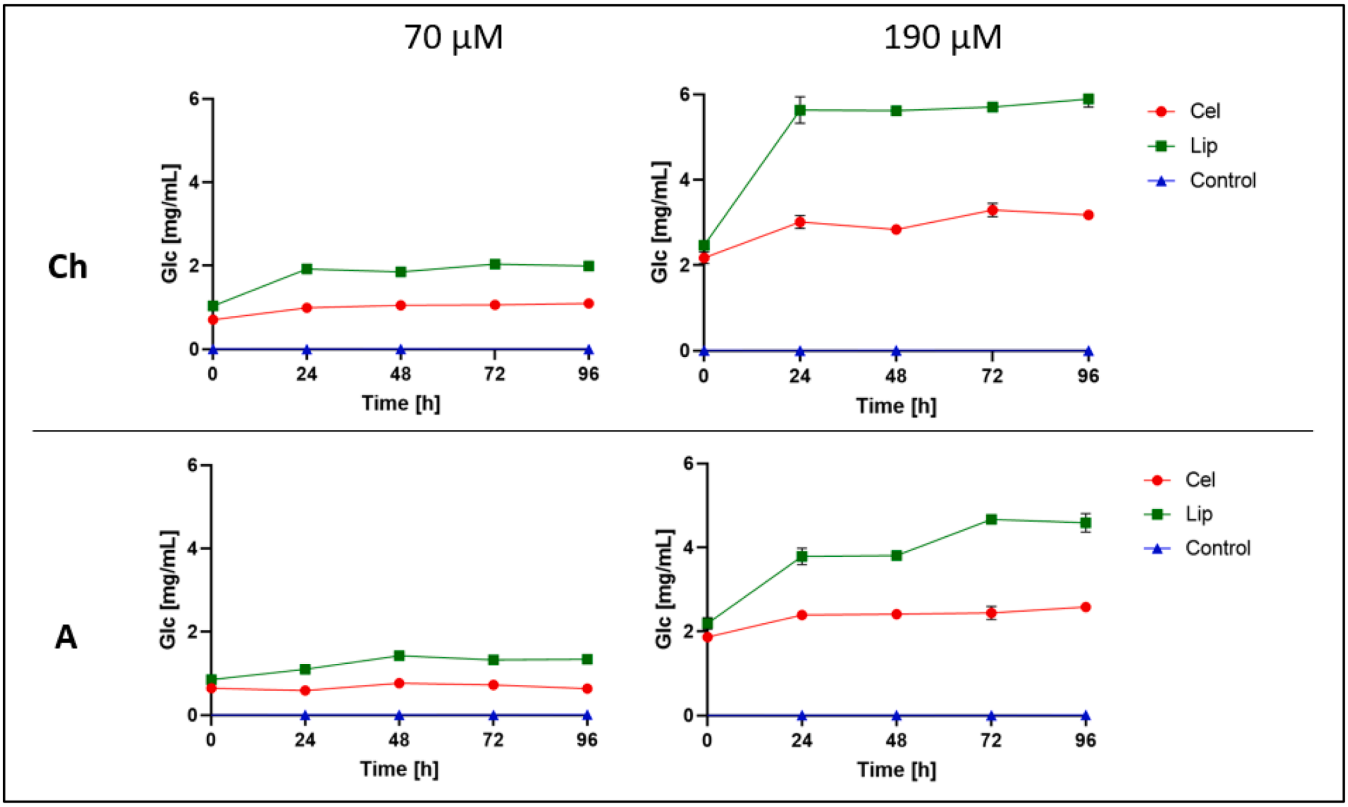

Fig. 7. Reducing sugar concentration after degradation of chitosan and alginate films with 70 μM and 190 μM lipase and cellulase at pH 6 in the presence of sodium azide. A – alginate film; Ch – chitosan film; Lip – lipase; Cel – cellulase. Variability is shown as standard deviation (error bars not visible for standard deviation below 10 %).

mL^{-1} with 190 μM Cel and Lip, respectively. For A-films, the maximum amount of reducing sugars was 0.7 mg mL^{-1} and 1.4 mg mL^{-1} with 70 μM

Cel and Lip after 48 h, respectfully. For 190 μM Cel, the maximum reducing sugar concentration of 2.4 mg mL^{-1} was reached after 48 h, but for 190 μM Lip, the maximum concentration of 4.7 mg mL^{-1} was reached after 72 h. We also observed a the very distinct structure of the Ch-films when comparing Cel and Lip reactions after the 96-hour incubation period (Fig. S5). The films that were incubated with Lip remained whole, whereas, the films that were incubated with Cel, broke down into small flakes, producing a while-coloured suspension.

Since no drop in reducing sugar concentration was measured when reaction mixtures contained NaAz, the most plausible interpretation is that the decrease observed in untreated mixtures was caused by residual microbial metabolism rather than by adverse side reactions such as repolymerization. Our results also show, that the maximum reducing sugar concentration was reached after 48 h and an extended incubation was not needed. This behaviour may arise from two factors: (i) a decrease in enzyme activity after 48 h, or (ii) exhaustion of accessible cleavage sites within the polymer, preventing further degradation. Moreover, the distinct structures of Ch-films after treatment with Lip or Cel, indicate substantial differences their depolymerization mechanisms.

Because depolymerization activity peaked at ~48 h, we investigated whether this was due to a general loss of enzyme activity or depletion of accessible cleavage sites within the polymer. Therefore, in the follow-up experiment Ch-films were incubated with 70 μM Lip or Cel for 48 h, after which the enzyme solution was removed, and a fresh enzyme solution was added to the remaining films or film fragments. These enzyme replenishment steps were performed in 4 cycles, and the amount of reducing sugars was measured for each one. NaAz was also added to the reaction mixture to prevent microbial growth. As shown in Fig. 8, the reducing sugar concentration was similar in all 4 cycles for both enzymes, confirming that the depolymerization of Ch-films is indeed limited due to loss of enzyme activity in 48 h under the tested conditions.

The different physical appearance of Ch-films after Lip and Cel treatment suggests that the two enzymes do not affect the film matrix in identical ways. However, the present data are insufficient to assign specific endo- versus exo-type pathways or to distinguish conclusively between monomer- and oligomer-dominated product mixtures. The replenishment experiment supports a simpler conclusion: fresh enzyme addition restored activity in successive cycles, which indicates that the plateau observed in single-batch reactions is governed mainly by loss of catalytic activity under the tested conditions, rather than by immediate exhaustion of all accessible cleavage sites.

3.3. Effects of film degradation products on plant growth and seed germination

After the soil and enzyme experiments, we assessed whether degradation of the films is associated with any obvious phytotoxic effects. Therefore, the effects on growth and seed germination of barley seeds were examined. Two experimental set ups were tested: one with pre-germinated sprouts, in which plant growth was monitored (Fig. 9a; Fig. S2), and one with directly sown seeds, in which both growth and germination were recorded (Fig. 9b). Across both assays, only minor differences relative to the control were observed.

Seed viability remained high in all film-treated groups. In the first experiment, A-based films increased plant size by 10 %, while A-CNC and A-mCNC decreased it by 6 % and 12 %, respectively. Ch-based films showed a minimal effect. Plant size was comparable to the control for Ch and Ch-CNC, and 7 % higher for Ch-mCNC. In the second experiment, where seeds were both germinated and grown on biocomposite films (Fig. 9b), their effects differed slightly. Plant size with A-mCNC was comparable to controls, while A and A-CNC films caused an 11 % and 8 % increase, respectively.

Ch-based films showed no effects on growth. The seed viability exceeded 97 % in all film samples except control and A-films, where it was 90 % and 87.5 %, respectively.

The small differences between the two experiments are most likely related to the different starting conditions. In the first experiment, similarly sized pre-germinated sprouts were selected, which reduced variability and excluded possible effects on germination itself. In the second experiment, germination and early growth occurred in the presence of the films, making the system more variable but also more environmentally relevant. Because only one plant species was tested and only gross endpoints (plant length and seed viability) were measured, these data should be interpreted as a preliminary screen for major inhibitory effects rather than a comprehensive ecotoxicological assessment. Within that scope, the results do not indicate major phytotoxicity of the film degradation products under the tested conditions.

Overall, the study has several important limitations that should be kept in mind. The soil assay was qualitative and based on visible disappearance rather than standardized mineralization; only one forest soil was examined; microbial community composition and soil enzyme activity were not characterized; ATR-FTIR and DNS provide indirect evidence of depolymerization; and the plant assay was limited to barley and a small number of endpoints. Future work should therefore include respirometric mineralization measurements, multi-soil validation, morphological analysis of hydrated residues, and product-resolved analyses such as SEC/GPC, LC-MS or NMR.

4. Conclusions

Under the tested native forest-soil microcosm conditions, all A- and Ch-based biocomposite films reached complete visible disappearance, with MID samples disappearing markedly faster than TOP samples. The results therefore support the environmental disintegration of these materials in soil, while not constituting a standardized mineralization assessment. Ch-based films disappeared faster than A-based films in the

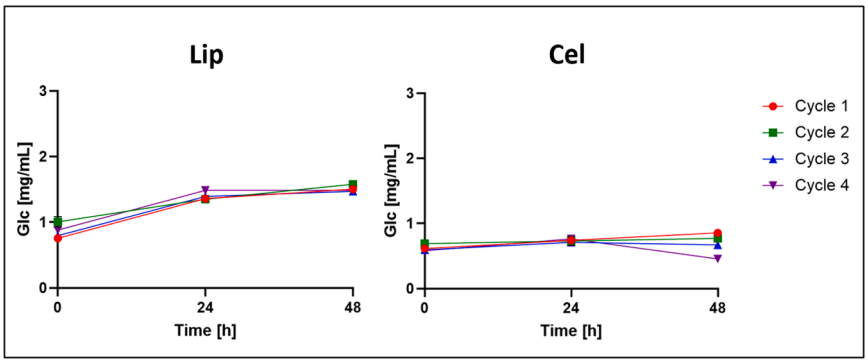

Fig. 8. Reducing sugar concentration after 4 cycles of degradation of chitosan films with 70 μM lipase and cellulase at pH 6 in the presence of sodium azide. Ch – chitosan film; Lip – lipase; Cel – cellulase. Variability is shown as standard deviation (error bars not visible for standard deviation below 10 %).

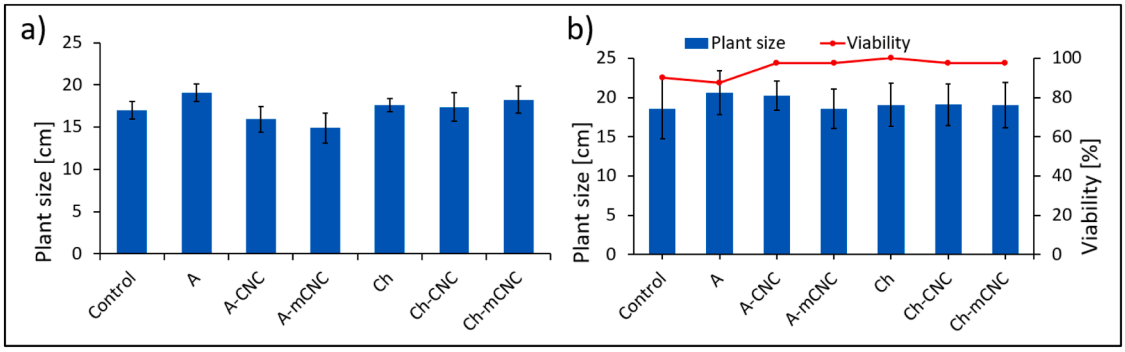

Fig. 9. Plant size and viability of seeds grown on soil (control) or soil with alginate and chitosan films. a) Plant size pre-germinated seeds grown on soil or soil with alginate and chitosan films; b) Plant size and viability of seeds germinated and grown on soil or soil with alginate and chitosan films. A – alginate film; A-CNC – alginate film with cellulose nanocrystals; A-mCNC - alginate film with modified cellulose nanocrystals; Ch – chitosan film; Ch-CNC – chitosan film with cellulose nanocrystals; Ch-mCNC – chitosan film with cellulose nanocrystals.

TOP set-up, which may reflect differences in hydration behaviour and the broad occurrence of terrestrial microorganisms capable of attacking chitin/chitosan-like substrates. In vitro assays showed that Lip and Cel generated the highest release of reducing sugars from the films, whereas Lac and ADH had negligible effects under the tested conditions. ATR-FTIR of Ch-based films revealed spectral changes consistent with chemical modification/depolymerization, but not definitive proof of specific bond scission. The plant screening assay showed no major inhibitory effects on barley germination or growth. Taken together, these results support A- and Ch-based CNC-containing films as promising biodegradable alternatives for transient applications, while underscoring the importance of soil conditions, matrix accessibility and analytical scope when interpreting biodegradation behaviour.

CRediT authorship contribution statement

Miša Mojca Cajnko: Writing – review & editing, Writing – original draft, Methodology, Funding acquisition, Formal analysis, Conceptualization. **Kostadin Mitkov:** Writing – original draft, Methodology. **Blaž Likozar:** Supervision, Resources. **Blaž Stres:** Writing – review & editing, Supervision, Methodology, Formal analysis, Conceptualization.

Declaration of competing interest

The authors declare that they have no known competing financial interests or personal relationships that could have appeared to influence the work reported in this paper.

Acknowledgements

This research was funded by the Slovenian Research and Innovation Agency within the project J4-50148 and P2-0152.

Supplementary materials

Supplementary material associated with this article can be found, in the online version, at doi:10.1016/j.carpta.2026.101166.

Data availability

No data was used for the research described in the article.

References

Abou-Zeid, D. M., Müller, R. J., & Deckwer, W. D. (2001). Degradation of natural and synthetic polyesters under anaerobic conditions. *Journal of Biotechnology, 86*, 113–126. https://doi.org/10.1016/S0168-1656(00)00406-5

Camiña, F., Trasar-Cepeda, C., Gil-Sotres, F., & Leirós, C. (1998). Measurement of dehydrogenase activity in acid soils rich in organic matter. *Soil Biology & Biochemistry, 30*, 1005–1011. https://doi.org/10.1016/S0038-0717(98)00010-8

Crognale, S., Russo, C., Petruccioli, M., & D'Annibale, A. (2022). Chitosan production by Fungi: Current State of knowledge. *Future Opportunities and Constraints, Fermentation, 8*, 76. https://doi.org/10.3390/fermentation8020076

Dong, Y., Gao, M., Song, Z., & Qiu, W. (2020). Microplastic particles increase arsenic toxicity to rice seedlings. *Environ. Pollut., 259*, Article 113892. https://doi.org/10.1016/J.ENVPOL.2019.113892

Fashogbon, R. O., Adebayo, B., Musa, V., & Femi-Ola, T. (2021). Lipolytic Activities of Bacteria and Fungi Isolated from Soil Samples. *Microbiol. Res. J. Int.*, 27–43. https://doi.org/10.9734/MRJI/2021/V31I530318

Food and Agriculture Organization, Standard operating procedure for soil pH determination, Rome, 2021. ttps://openknowledge.fao.org/server/api/core/bitstreams/6ad6862a-eadc-437c-b359-ef14cb687222/content.

Fujisawa, M., Hirai, H., & Nishida, T. (2001). Degradation of polyethylene and nylon-66 by the Laccase-Mediator system. *Journal of Polymers and the Environment, 9*(9), 103–108. https://doi.org/10.1023/A:1020472426516, 2001.

Gajendiran, A., Krishnamoorthy, S., & Abraham, J. (2016). Microbial degradation of low-density polyethylene (LDPE) by Aspergillus clavatus strain JASK1 isolated from landfill soil. *3 Biotech, 6*, 1–6. https://doi.org/10.1007/S13205-016-0394-X

Gu, Y., Wang, P., & Kong, C. H. (2009). Urease, invertase, dehydrogenase and polyphenoloxidase activities in paddy soil influenced by allelopathic rice variety. *European Journal of Soil Biology, 45*, 436–441. https://doi.org/10.1016/j.ejsobi.2009.06.003

Guzmán-Pincheira, C., Moeini, A., Oliveira, P. E., Abril, D., Paredes-Padilla, Y. A., & Benavides-Valenzuela, S. (2025). Development of Alginate-Chitosan bioactive films containing essential oils for use in food packaging. *Foods, 14*, 256. https://doi.org/10.3390/foods14020256

Hernández-López, A., Sánchez Félix, D. A., Zuñiga Sierra, Z., García Bravo, I., Dinkova, T. D., & Avila-Alejandre, A. X. (2020). Quantification of reducing sugars based on the qualitative technique of Benedict. *ACS Omega, 5*, 32403–32410. https://doi.org/10.1021/acsomega.0c04467

Huafei, X., Zhengyu, J., Jinhui, H., & Cuirong, Z. (2024). Preparation of low molecular weight chitosan by complex enzymes hydrolysis. *International Journal of Chemistry, 3*, 180. https://doi.org/10.5539/ijc.v3n2p180

Hung, C. S., Zingarelli, S., Nadeau, L. J., Biffinger, J. C., Drake, C. A., Crouch, A. L., Barlow, D. E., Russell, J. N., & Crookes-Goodson, W. J. (2016). Carbon catabolite repression and impranil polyurethane degradation in Pseudomonas protegens strain pf-5. *Applied and Environmental Microbiology, 82*, 6080–6090. https://doi.org/10.1128/AEM.01448-16

Isangedighi, I. A., David, G. S., & Obot, O. I. (2020). Plastic waste in the aquatic environment : Impacts and management, Anal. *Nanoplastics Microplastics Food*, 15–43. https://doi.org/10.1201/9780429469596-2

Kaczyńska, G., Borowik, A., & Wyszkowska, J. (2015). Soil dehydrogenases as an indicator of contamination of the environment with petroleum products. *Water, Air, & Soil Pollution, 226*, 372. https://doi.org/10.1007/s11270-015-2642-9

Kim, H. R., Lee, H. M., Yu, H. C., Jeon, E., Lee, S., Li, J., & Kim, D. H. (2020). Biodegradation of polystyrene by Pseudomonas sp. Isolated from the gut of superworms (Larvae of Zophobas atratus). *Environmental Science & Technology, 54*, 6987–6996. https://doi.org/10.1021/ACS.EST.0C01495

Kumar, M. N. V. R., Muzzarelli, R. A. A., Muzzarelli, C., Sashiwa, H., & Domb, A. J. (2004). Chitosan chemistry and Pharmaceutical perspectives. *Chemical Reviews, 104*, 6017–6084. https://doi.org/10.1021/cr030441b

Li, S., Ren, Y., Hou, Y., Zhan, Q., Jin, P., Zheng, Y., & Wu, Z. (2024). Polysaccharide-based composite films: Promising biodegradable food packaging materials. *Foods, 13*, 3674. https://doi.org/10.3390/foods13223674

Metha, C., Pawar, S., & Suvarna, V. (2024). Recent advancements in alginate-based films for active food packaging applications, Sustain. *Food Technology, 2*, 1246–1265. https://doi.org/10.1039/D3FB00216K

Mukherjee, K., Tribedi, P., Chowdhury, A., Ray, T., Joardar, A., Giri, S., & Sil, A. K. (2011). Isolation of a Pseudomonas aeruginosa strain from soil that can degrade

polyurethane diol. *Biodegradation, 22*, 377–388. https://doi.org/10.1007/S10532-010-9409-1

Oberlintner, A., Likozar, B., & Novak, U. (2023). Effect of environment on acetylated cellulose nanocrystal-reinforced biopolymers films. *Polymers, 15*, 1663. https://doi.org/10.3390/polym15071663

Paques, J. P., van der Linden, E., van Rijn, C. J. M., & Sagis, L. M. C. (2014). Preparation methods of alginate nanoparticles. *Advances in Colloid and Interface Science, 209*, 163–171. https://doi.org/10.1016/j.cis.2014.03.009

Pathak, V. M., & Navneet. (2017). Review on the current status of polymer degradation: A microbial approach. *Bioresources and Bioprocessing, 4*(4), 1–31. https://doi.org/10.1186/S40643-017-0145-9, 2017.

Poshina, D. N., Raik, S. V., Poshin, A. N., & Skorik, Y. A. (2018). Accessibility of chitin and chitosan in enzymatic hydrolysis: A review. *Polymer Degradation and Stability, 156*, 269–278. https://doi.org/10.1016/j.polymdegradstab.2018.09.005

Rinta-Kanto, J. M., Sinkko, H., Rajala, T., Al-Soud, W. A., SØrensen, S. J., Tamminen, M. V., & Timonen, S. (2016). Natural decay process affects the abundance and community structure of bacteria and archaea in Picea abies logs. *FEMS Microbiology Ecology, 92*, fiw087. https://doi.org/10.1093/FEMSEC/FIW087

Rosenboom, J. G., Langer, R., & Traverso, G. (2022). Bioplastics for a circular economy. *Nature Reviews. Materials, 7*(7), 117–137. https://doi.org/10.1038/s41578-021-00407-8, 2022.

Ryo, K., Kodai, M., Shota, K., Shojiro, H., Rui, K., Miki, N., Yudai, H., Eugene, K., T, B. G., Naofumi, K., & Eiji, M. (2023). Stereoinversion via alcohol dehydrogenases enables complete catabolism of β-1-type lignin-derived aromatic isomers. *Applied and Environmental Microbiology, 89*, Article e00171-23. https://doi.org/10.1128/aem.00171-23

Saqib, A. A. N., & Whitney, P. J. (2011). Differential behaviour of the dinitrosalicylic acid (DNS) reagent towards mono- and di-saccharide sugars. *Biomass and Bioenergy, 35*, 4748–4750. https://doi.org/10.1016/j.biombioe.2011.09.013

Sethi, S., Datta, A., Gupta, B. L., & Gupta, S. (2013). Optimization of cellulase production from bacteria isolated from soil. *Int Sch Res Not, 2013*, 1–7. https://doi.org/10.5402/2013/985685

Sidari, R., Pittarello, M., Rodinò, M. T., Panuccio, M. R., Lo Verde, G., Laudicina, V. A., & Gelsomino, A. (2025). Isolation and selection of cellulose-chitosan degrading bacteria to speed up the mineralization of bio-based mulch films. *Front Microbiol Volume, 16*. https://www.frontiersin.org/journals/microbiology/articles/10.3389/fmicb.2025.1597786.

Stapleton, P. A. (2019). Toxicological considerations of nano-sized plastics. *AIMS Environmental Science, 6*, 367–378. https://doi.org/10.3934/ENVIRONSCI.2019.5.367/FULLTEXT.HTML

Vaksmaa, A., Knittel, K., Abdala Asbun, A., Goudriaan, M., Ellrott, A., Witte, H. J., Vollmer, I., Meirer, F., Lott, C., Weber, M., Engelmann, J. C., & Niemann, H. (2021). Microbial communities on plastic polymers in the Mediterranean Sea. *Frontiers in Microbiology, 12*, 1021. https://doi.org/10.3389/FMICB.2021.673553/BIBTEX

Vidmar, B., Oberlintner, A., Stres, B., Likozar, B., & Novak, U. (2023). Biodegradation of polysaccharide-based biocomposites with acetylated cellulose nanocrystals, alginate and chitosan in aqueous environment. *International Journal of Biological Macromolecules, 252*, Article 126433. https://doi.org/10.1016/j.ijbiomac.2023.126433

Xia, W., Liu, P., & Liu, J. (2008). Advance in chitosan hydrolysis by non-specific cellulases. *Bioresource Technology, 99*, 6751–6762. https://doi.org/10.1016/j.biortech.2008.01.011

Xie, F., Gao, C., & Avérous, L. (2024). Alginate-based materials: Enhancing properties through multiphase formulation design and processing innovation. *Mater Sci Eng R Reports, 159*, Article 100799. https://doi.org/10.1016/j.mser.2024.100799

Yoon, M. G., Jeon, H. J., & Kim, M. N. (2012). Biodegradation of polyethylene by a soil bacterium and AlkB cloned recombinant cell. *J Bioremediation Biodegrad, 03*(3), 1–8. https://doi.org/10.4172/2155-6199.1000145, 2012.

Zhao, Y., Xiang, W., Ma, M., Zhang, X., Bao, Z., Xie, S., & Yan, S. (2019). The role of laccase in stabilization of soil organic matter by iron in various plant-dominated peatlands: Degradation or sequestration? *Plant and Soil, 443*, 575–590. https://doi.org/10.1007/s11104-019-04245-0